Catalysis Science & Technology

www.rsc.org/catalysis

Volume 2 | Number 6 | June 2012 | Pages 1075–1294

ISSN 2044-4753

RSC Publishing

COVER ARTICLE

Debecker, Mutin *et al.*

A non-hydrolytic sol–gel route to highly active MoO_3–SiO_2–Al_2O_3 metathesis catalysts

2044-4753(2012)2:6;1-9

Catalysis
Science & Technology

Cite this: *Catal. Sci. Technol.*, 2012, **2**, 1157–1164

www.rsc.org/catalysis

PAPER

A non-hydrolytic sol–gel route to highly active MoO_3–SiO_2–Al_2O_3 metathesis catalysts†

Damien P. Debecker,*[a] Karim Bouchmella,[b] Mariana Stoyanova,[c] Uwe Rodemerck,[c] Eric M. Gaigneaux[a] and P. Hubert Mutin*[b]

Received 21st November 2011, Accepted 21st December 2011
DOI: 10.1039/c2cy00475e

MoO_3-based materials are known to be appropriate catalysts for the heterogeneous metathesis of light olefins. Classical preparation methods involve the deposition of a Mo oxide phase on the surface of preformed support *via* impregnation, grafting or thermal spreading. An alternative sol–gel approach for the elaboration of Mo-based catalysts is presented in this article. Mesoporous ternary Si–Al–Mo mixed oxides are prepared in one step, *via* non-hydrolytic condensation of chloride precursors in non-aqueous media. After calcination, effective catalysts with very good textures and highly dispersed surface molybdenum species are obtained. The Si/Al ratio influences both the texture and the acidity of the materials, which significantly affects the propene self-metathesis activity. The activity also increases with the MoO_3 content. The best catalysts with optimized composition significantly outperform the catalysts prepared by other methods.

1. Introduction

The metathesis of light olefins is a crucial reaction for the petro-chemical industry as it allows the conversion of low-value alkenes (or alkenes produced in excess in the refinery) into more demanded ones.[1] Historically, the metathesis reaction was discovered when propene was reacted on supported MoO_3 catalysts and the production of ethene, *cis*-2-butene and *trans*-2-butene was observed.[2] It was then found that supported W and Re oxides can also catalyse the self-metathesis of propene. The reaction is athermal and reversible. Nowadays, the reverse reaction (cross-metathesis of ethene and butene) is of particular interest because propene is highly demanded in the market.[3]

The self-metathesis of propene is a convenient model reaction largely used to evaluate the metathesis activity of heterogeneous catalysts. Recent works on MoO_3-based metathesis catalysts have highlighted their high activity, especially if supported on silica–alumina.[4–7] MoO_3/SiO_2–Al_2O_3 catalysts, as opposed to MoO_3/SiO_2 or MoO_3/Al_2O_3 catalysts, develop a surface acidity which is beneficial to the reaction.[4,5] In addition, the superior activity of highly dispersed Mo species was supported by many experimental data.[8–10] Consequently, much effort has been directed toward finding preparation methods which promote the stabilization of highly dispersed MoO_x species at the surface of silica–alumina.

Traditional catalyst preparation methods (impregnation, thermal spreading, grafting) usually consist of two-step procedures in which the support—prepared in the first step—is covered by the active phase in the second step. This strategy implies limitations such as the non-uniform deposition of the active phase (*e.g.* not deposited inside the pores of the support[11]), the formation of inactive species (*e.g.* $Al_2(MoO_4)_3$ and MoO_3 crystals[11,12]) or the lack of interaction between the active phase and the support (*e.g.* incomplete spreading of MoO_3 *via* thermal spreading[13,14]). Impregnation methods can be improved somewhat by changing the nature of the Mo precursor, with the aim to increase the Mo dispersion, thereby increasing the activity.[9,15] Nevertheless, obtaining a molecular-scale dispersion of Mo species at the surface of a pre-existing support remains difficult. Recently, remarkable turn-over frequencies were reached with catalysts prepared *via* flame spray pyrolysis (FSP) because this method allows the production of highly dispersed species at low MoO_3 loading.[8] However, as the specific surface area remains relatively low with this method, the MoO_3 loading has to be kept very low (1 wt%) to prevent the formation of condensed molybdena phases, thus limiting the actual specific activity. Outstanding cross-metathesis activity was recently obtained with highly porous MoSiAl mixed oxides prepared *via* an aerosol-assisted sol–gel method,[16] showing again that

[a] *Institute of Condensed Matter and Nanoscience–MOlecules, Solids and reactiviTy (IMCN/MOST), Université catholique de Louvain, Croix du Sud 2/17, 1348 Louvain-La-Neuve, Belgium. E-mail: damien.debecker@uclouvain.be; Fax: +3210473649; Tel: +3210473648*
[b] *Institut Charles Gerhardt, UMR 5253, CNRS-UM2-ENSCM-UM1, Université Montpellier 2, cc 1701, Montpellier 34095, France. E-mail: hubert.mutin@univ-monpt2.fr; Fax: +334 6714 3852; Tel: +334 6714 4943*
[c] *Leibniz-Institut für Katalyse e.V. an der Universität Rostock, Albert-Einstein-Str. 29a, 18059 Rostock, Germany*
† Electronic supplementary information (ESI) available. See DOI: 10.1039/c2cy00475e

high specific surface area and good Mo dispersion are the decisive factors for the design of efficient metathesis catalysts.

In this context, a new one-step process based on a non-hydrolytic sol–gel route and leading to MoO_3–SiO_2–Al_2O_3 mixed oxides was proposed recently.[17] Preliminary catalytic assays showed that these materials were active catalysts for the self-metathesis of propene. The present paper presents a systematic approach to optimize the preparation method and reach high metathesis activity. The materials were obtained by the direct reaction of low-cost Mo, Si and Al chloride precursors with diisopropyl ether (see Experimental section). Two parameters of the preparation were screened: the Al_2O_3 and the MoO_3 contents. The physico-chemical properties of the solids produced were studied and correlated with the catalytic performance. Particular attention was devoted to the description of the MoO_x species and to the acidity of the solids.

The choice of the non-hydrolytic sol–gel route is justified by the difficulties encountered in the synthesis of mesoporous mixed oxides by conventional sol–gel processes. Such conventional sol–gel routes are based on the hydrolysis and condensation of molecular precursors, usually alkoxides.[18–21] However, in the case of SiO_2-based mixed oxides, the very different reaction rates of metal and silicon precursors make the simultaneous control of composition, structure and texture of the gels problematic. Thus, complicated experimental procedures are required to prepare homogeneous mesoporous materials, including prehydrolysis of the less reactive precursors or modification with chelating agents of the more reactive ones, and low-temperature extraction with supercritical CO_2 (aerogels).[22] Conversely, non-hydrolytic routes[23] based on the reaction of chloride precursors with alkoxide precursors or diisopropyl ether were shown to provide an excellent control over the stoichiometry and the homogeneity of mixed oxide gels. Furthermore, the generally high degree of condensation of non-hydrolytic gels allows the formation of mesoporous xerogels with high surface area and pore volumes after simple evaporative drying, thus avoiding the supercritical drying step.[24] Accordingly, these non-hydrolytic routes are attracting increasing attention for the preparation of mixed oxide catalysts.[25–33]

2. Results

In this study, two parameters of the catalysts preparation have been varied systematically: the alumina content (in other words, the Si/Al ratio) and the MoO_3 content. The samples are labelled NH_Y_X, where NH stands for "non-hydrolytic sol–gel", Y represents the Al_2O_3 content (in wt%) and X represents the MoO_3 content (in wt%). The effect of these parameters on the texture and acidity of the solids was correlated to their catalytic activity in the metathesis of propene.

A first set of ten samples (Table 1, first ten entries) with various Si/Al ratios and a constant MoO_3 content was examined with the aim to identify the most appropriate Al_2O_3 content. The MoO_3 content was kept constant at 10 wt%. The range of SiO_2/Al_2O_3 ratio explored varied from infinite (no alumina in NH_0_10) to zero (no silica in NH_90_10). Then, mixed oxides with the most promising Si/Al ratio (Si/Al $\approx$ 17) and various MoO_3 contents ranging from 5 to 20 wt% were examined in a search for higher catalytic performances (Table 1, last four entries).

Table 1 Composition and textural properties (N_2-physisorption) of the samples with variable Al_2O_3 and MoO_3 contents

Sample	Composition SiO_2 : Al_2O_3 : MoO_3 (wt%)[a]	SSA/ $m^2\ g^{-1}$	V_p/ $cm^3\ g^{-1}$	D_p/ nm	SSAμ/ $m^2\ g^{-1}$
NH_0_10	90.3 : 0.0 : 9.7	740	1.1	5.8	70
NH_5_10a	83.9 : 5.4 : 10.7	520	1.5	12.0	40
NH_10_10	79.9 : 10.0 : 10.1	330	0.6	7.8	30
NH_15_10	74.0 : 15.4 : 10.5	200	0.3	6.5	30
NH_20_10	68.8 : 19.4 : 11.8	190	0.3	6.7	30
NH_25_10	64.5 : 25.4 : 10.1	210	0.3	6.2	26
NH_45_10	44.2 : 45.5 : 10.3	320	0.4	5.3	59
NH_65_10	26.3 : 62.9 : 10.8	290	0.2	3.3	100
NH_80_10	10.6 : 78.9 : 10.5	260	0.1	2.2	130
NH_90_10	0.0 : 89.5 : 10.5	480	0.6	5.1	—
NH_5_5	90.3 : 5.2 : 4.6	500	0.9	7.2	40
NH_5_10b	86.4 : 4.1 : 9.5	480	1.6	13.1	20
NH_5_15	79.9 : 4.7 : 15.4	470	1.6	13.3	0
NH_5_20	77.0 : 4.2 : 18.8	490	1.6	13.3	10

[a] Determined by ICP-OES and considering that all Si, Al and Mo atoms are in the form of SiO_2, Al_2O_3 and MoO_3 respectively.

2.1. Composition and texture of MoO_3–SiO_2–Al_2O_3 catalysts prepared by non-hydrolytic sol–gel

ICP-OES results showed that the final composition of the Mo–Si–Al mixed oxides prepared by non-hydrolytic sol–gel was always very close to the nominal one (Table 1). This means that no metallic species were lost in the liquid phase or in the gas phase during the drying and calcination steps. The reliability of the synthesis in terms of sample composition was also demonstrated for other catalytic systems.[32,33]

Nitrogen physisorption indicated that the SiO_2–MoO_3 (NH_0_10) and Al_2O_3–MoO_3 (NH_90_10) samples were mesoporous with type IV isotherms (according to the BDDT classification) typical of mesoporous solids (see Fig. S1, ESI†) and specific surface areas (SSA) of 740 $m^2\ g^{-1}$ (NH_0_10) and 480 $m^2\ g^{-1}$ (NH_90_10) (Table 1). Conversely, the SiO_2–Al_2O_3–MoO_3 catalysts exhibited Type II isotherms, except NH_80_10 which was mainly microporous with a type I isotherm (Fig. 1). The NH_5_X samples with a 5 wt% alumina content and various MoO_3 loadings all showed similar specific surface areas around 500 $m^2\ g^{-1}$ and high pore volumes (V_p), from 0.9 to 1.6 $cm^3\ g^{-1}$. Thus, the MoO_3 content had no significant impact on the texture (see Fig. S2, ESI†). The samples with higher alumina contents had significantly lower surface areas (from 190 to 330 $m^2\ g^{-1}$) and pore volumes (from 0.1 to 0.6 $cm^3\ g^{-1}$). *t*-Plot analysis indicated that the surface area developed by micropore walls (denoted SSAμ in Table 1) was low, except for the catalysts with a high alumina content (NH_65_10 and NH_80_10). Average pore diameter (D_p) ranged between 5 and 14 nm. TEM micrographs showed highly porous particles, with polydispersed and apparently interconnected pores (Fig. 2).

2.2. Structural characterization and surface acidity

2.2.1. XRD and Raman. The XRD patterns of the NH samples presented in all cases a halo around 20–25° typical of amorphous solids (Fig. S4, ESI†). There was no evidence of crystalline molybdenum oxide in the XRD patterns of the sol–gel samples, showing that no MoO_3 crystallites larger than the detection limit—about 5 nm[34]—were present. The only

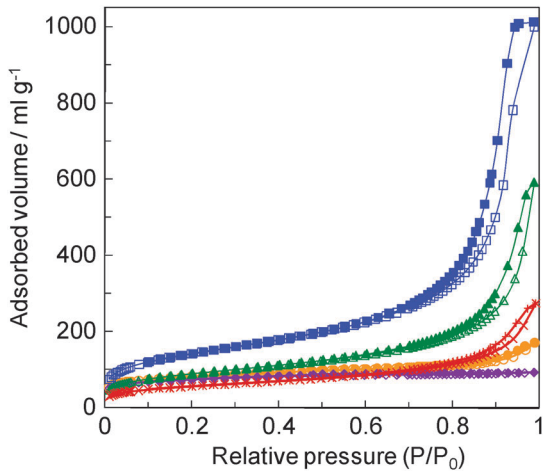

Fig. 1 N_2 adsorption–desorption isotherms for SiO_2–Al_2O_3–MoO_3 samples. (■, □) NH_5_10 adsorption and desorption respectively, (▲, Δ) NH_10_10, (×, +) NH_15_10, (●, ○) NH_65_10 and (♦, ◊) NH_80_10. The isotherms of NH_20_10, NH_25_10 and NH_45_10 catalysts are very similar to those of NH_15_10 and are not shown for the sake of clarity of the figure (see Fig. S3, ESI†).

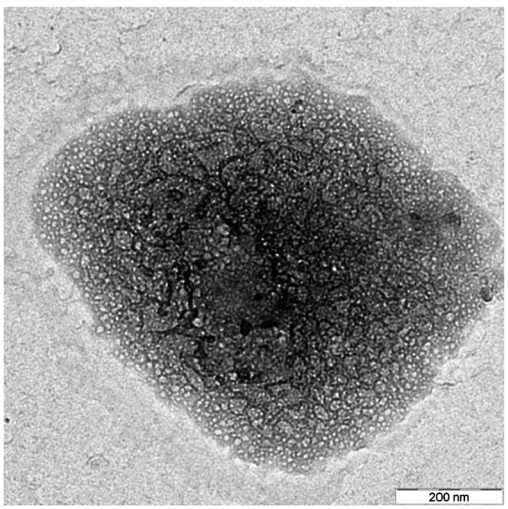

Fig. 2 Transmission electron micrograph of the NH_5_10 sample (scale bar = 200 nm).

exception concerned the sample with the highest MoO_3 content (NH_5_20)[17] for which a small diffraction line at 27.5° indicated the presence of traces of crystalline MoO_3 (JCPDS 05-0508).

Raman spectroscopy was tentatively used to characterize the MoO_x species present in the solids. However, the background of the spectra, originating from complex vibration modes of the silica–alumina matrix and from a broad and intense signal presumably due to the fluorescence of impurities made the observation of MoO_x species complicated. Fig. 3 shows that for the silica-rich samples the intensity of the background increased with the alumina content, coherent with the increasing amount of defects in the structure of the silica–alumina matrix as the Al content increased. Thus, in Al-containing samples, dispersed and amorphous molybdenum species with weak Raman response[35] were not observable. Such fluorescence problems could possibly be minimized using another excitation source or analysing the

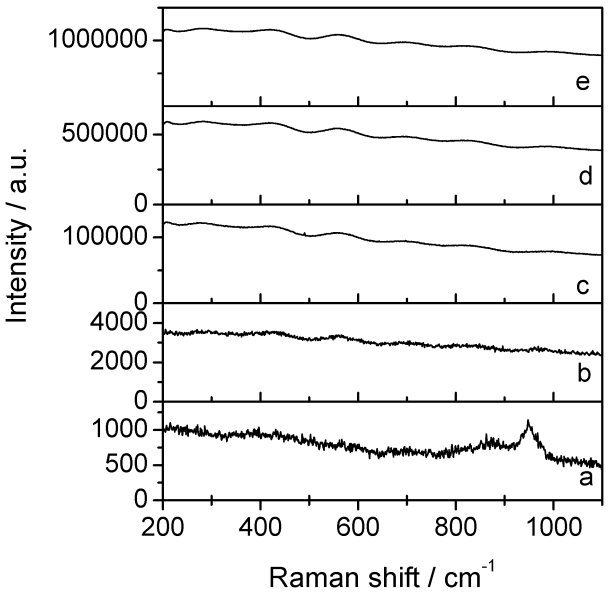

Fig. 3 Raman spectra of (a) NH_0_10, (b) NH_5_10, (c) NH_10_10, (d) NH_15_10 and (e) NH_20_10. The scale of the left axis changes from one spectrum to another and shows that the intensity of the background increases when the Al content increased.

sample under dehydrated conditions.[8,36] In the conditions used here, however, it can already be stressed that no bands related to crystalline MoO_3 species were detected in any spectra (signals expected at 996, 819 and 666 cm^{-1}[37]), even though such crystalline species are known to be strong Raman scatterers compared to amorphous and dispersed species. In similar samples with strong fluorescence background and analysed under similar conditions, small amounts of crystalline Mo oxide (even small crystallites) were easily detected (*e.g.* in MoO_3/SiO_2–Al_2O_3 catalysts prepared *via* wet impregnation[11] or thermal spreading[13]). So from Raman spectroscopy the presence of MoO_3 crystallites can be discarded for catalysts prepared by non-hydrolytic sol–gel. The NH_0_10 catalyst is the only sample for which the background was not too intense and for which two broad bands could be distinguished. Their maxima appear around 945–950 cm^{-1} and 871–878 cm^{-1}. The most intense peak is classically attributed to the stretch vibration of terminal Mo═O groups in amorphous polymeric MoO_x species,[37,38] while the other band is attributed to the stretch vibration of Mo–O–Mo bonds in polymers of octahedral MoO_6 units[39] or to isolated tetrahedrally coordinated Mo atoms.[38]

2.2.2. NH_3-TPD. Temperature programmed desorption of ammonia (NH_3-TPD) was used to probe the acidity of the NH catalysts (Table 2). The presence of medium or strong acidic sites appeared related to the presence of Al. The thermogram obtained for NH_0_10 (0% Al_2O_3) showed a broad desorption profile centred at 205 °C indicating the presence of weak acidic sites only.[40] Conversely, the thermograms of all of the Al-containing samples showed that ammonia desorbed up to 500 °C, indicating the presence of acidic sites with higher strength (see Fig. S5, ESI†). Their acidity was intermediate between the weakly acidic sites of silica and the highly acidic sites found in zeolites.[41] In order to estimate the relative amounts of weak and medium-strong sites, we used the method

Table 2 Acidity measured by NH_3-TPD

Sample	NH_3 desorbed/ mmol g^{-1}	Density of acid site/ nm^{-2}	Density of weak sites[a]/ nm^{-2}	Density of medium + strong sites[a]/nm^{-2}
NH_0_10	0.5	0.4	0.4 (100%)	0 (0%)
NH_5_10a	0.5	0.6	0.5 (82%)	0.1 (18%)
NH_5_20	0.8	1.0	0.8 (79%)	0.1 (28%)
NH_10_10	0.9	1.6	1.0 (58%)	0.7 (42%)
NH_15_10	0.9	2.7	1.4 (51%)	1.3 (49%)
NH_20_10	0.8	2.5	1.5 (61%)	1.0 (39%)
NH_25_10	0.8	2.3	1.1 (49%)	1.2 (51%)
NH_45_10	1	1.9	1.5 (79%)	0.4 (21%)
NH_65_10	1.2	2.5	1.4 (55%)	1.1 (45%)
NH_80_10	1	2.3	1.3 (56%)	1.0 (44%)
NH_90_10	0.6	0.8	0.7 (90%)	0.1 (10%)

[a] In brackets is given the percentage of each type of sites.

of Katada *et al.*:[40] a Gaussian function centred at *ca.* 205 °C was fitted to the peak and attributed to weak acidic sites. The rest of the peak was attributed to medium and strong acidic sites. Table 2 gives the total amount of ammonia desorbed from each sample, as well as the density of acidic sites derived from this value and from the specific surface area of each catalyst. The silica-based sample had the lowest density of acid sites and exhibited only weak sites. All other catalysts containing alumina exhibited also medium and strong sites. The density of acidic sites (acidity normalized by the specific surface area) increased with the alumina content up to 15–25 wt% and then tended to decrease for higher alumina contents. The same observation can be made concerning the acidity strength.

2.3. Metathesis activity

The samples were tested in the self-metathesis of propene at 40 °C (Fig. 4). All samples catalyzed the conversion of propene to ethene and butene with ~99% selectivity. The catalyst activity appeared to be highly dependent on the alumina and on the MoO_3 contents. For some samples, the activity increased during the first 20 minutes of the reaction and then slow deactivation took place. For some other samples, no activation period was observed and deactivation started from the beginning of the reaction.

The activity of the samples with a constant 10 wt% MoO_3 content strongly depended on the alumina content. The ternary catalysts with high alumina content (NH_65_10 and NH_80_10) as well as the binary samples (NH_90_10 and NH_0_10) showed low activities and relatively fast deactivation, in agreement with previous observations.[4] The ternary catalysts with intermediate alumina content (from 5 to 45 wt%) were more active, the best catalyst being the one with only 5 wt% of Al_2O_3. The activity of the NH_5_X samples increased with the MoO_3 charge.

The specific metathesis activity (taken at 14 min on stream) of the different NH catalysts is compared in Fig. 5. In terms of activity per gram of catalyst, the best catalysts in the NH_X_10 series were those with alumina content ranging from 5 to 45 wt%. The specific activity of the samples with no alumina or high alumina contents was much lower. The specific activity of the NH_5_X samples increased roughly linearly with the MoO_3 content, reaching the very high specific activity of ~45 mmol g^{-1} h^{-1} for NH_5_20.

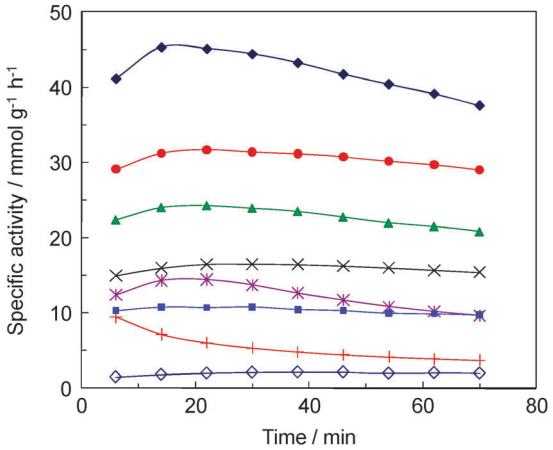

Fig. 4 Specific metathesis activity *versus* time on stream. The effect of the alumina content can be visualized within the series: (+) NH_0_10, (▲) NH_5_10, (×) NH_10_10, (*) NH_25_10, (◊) NH_90_10. For the sake of clarity, the activity of NH_65_10 and NH_80_10 (lower than that of NH_0_10) and the activity of NH_15_10 and NH_20_10 (curves similar to NH_10_10) are not shown. The effect of the MoO_3 content can be visualized within the series: (■) NH_5_5, (▲) NH_5_10, (●) NH_5_15 and (♦) NH_5_20. Reaction carried out with 200 mg of catalyst (100 mg only for NH_5_15 and NH_5_20 to remain far enough from thermodynamic equilibrium) at 40 °C, in a propene and N_2 flow (90 : 10 vol.%) of 8 ml min^{-1}, after activation at 550 °C under N_2.

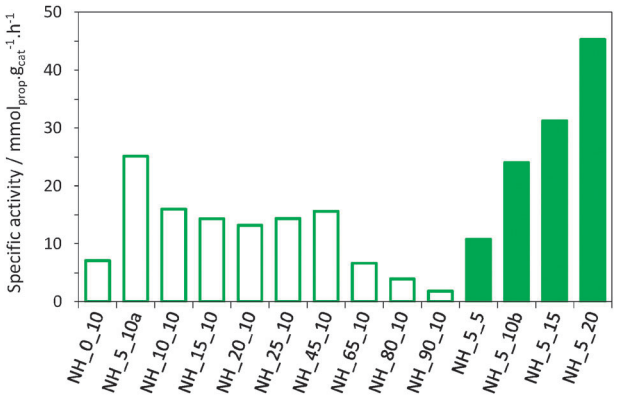

Fig. 5 Specific metathesis activity after 14 min on stream. Empty bar shows the influence of the alumina content. Full bar shows that the metathesis activity increases linearly with the MoO_3 content. NH_5_10a and NH_5_10b exhibited very similar activity (24 and 25 mmol g^{-1} h^{-1} respectively), showing that the preparation method is reproducible.

3. Discussion

3.1. Composition, texture, structure and acidity of the catalysts

Non-hydrolytic sol–gel provides a simple one-step route to mesoporous MoO_3–SiO_2–Al_2O_3 materials with relatively high surface areas and pore volumes. The specific surface area is maximum for the silica–molybdena catalyst, and then it decreases markedly upon introduction of 5 and 10 wt% alumina, and remains roughly constant for higher alumina contents. This effect seems to be intrinsic to silica–alumina based systems, regardless of the preparation method.[42–44]

Thus, the samples with a low alumina content (*ca.* 5 wt%) presented the best textures, with specific surface area around 500 m^2 g^{-1} and very high pore volumes (0.9–1.6 cm^3 g^{-1}). Conversely, the alumina-rich samples offered less interesting textures, with lower pore volume and a significant proportion of micropores.

According to Raman spectroscopy and XRD, all samples appeared amorphous. This is encouraging, since MoO_3 crystals were identified as inactive in the olefin metathesis.[4,11,45] The absence of MoO_3 crystals in silica-rich samples and particularly NH_0_10 (no alumina) is noteworthy, as it is well recognized that bulky molybdenum oxide crystals usually tend to form during calcination in MoO_3/SiO_2 catalysts prepared *via* classical methods.[38] The preferential formation of Mo–O–Mo bridges instead of Mo–O–Si bonds has been ascribed to the fact that both silica and molybdena are acidic, resulting in weak interactions between both materials,[46] so that calcination usually leads to sintering and formation of crystalline species. This process seems avoided here.

The catalytic activity of supported molybdenum oxide metathesis catalysts is known to be strongly influenced by the nature of the support[4–6,47] and the high activity of catalysts supported on silica–alumina has been ascribed to the acidic character of the support. In the present study, the composition of the samples has a marked influence on the acidity of the samples. The Al-free catalyst is the least acidic in terms of both the absolute amount and the density of acidic sites. Furthermore, it only exhibits weak acidity. As Al is introduced in silica-rich formulations, the density of both weak and medium/strong acidic sites increases and reaches a maximum for alumina contents of 15–25 wt%.

3.2. Correlation with metathesis activity

To take into account the differences in specific surface area or MoO_3 content of the catalysts, we plotted in Fig. 6 the specific activity normalized to the specific surface area ("areal activity" in mmol of propene converted per square metre of catalyst and per hour) and the apparent turnover frequency ("TOF" in mmol of propene converted per mole Mo and per second). On the basis of areal activity, the most active NH catalysts are the catalysts with 10 to 20 wt% Al_2O_3. The catalysts containing no alumina exhibit poor areal activity. Such a trend was previously reported for catalysts prepared by wet impregnation.[4] The samples with 65 to 90 wt% Al_2O_3 also showed poor areal activity, even though no significant difference was observed in terms of acidity with respect to other Al-containing samples. The very high specific activity (Fig. 4) of the NH_5_10 catalyst compared to the other NH_Y_10 catalysts with intermediate Al_2O_3 contents (10 to 45 wt%) can clearly be explained by a textural effect. The very low activity of NH_0_10 can be ascribed to the absence of medium/strong acidic sites in the silica matrix. On the other hand, the correlation between acidity, texture and activity in alumina containing catalysts is poor. In particular, the relatively low activity of the samples with high alumina content cannot be directly correlated to differences in texture or surface acidity. Possibly, the nature of the Mo surface sites is affected by the high alumina content, as it is well known that Mo can interact strongly with alumina (to form aluminium molybdates, for instance) while the interaction with silica is poor.

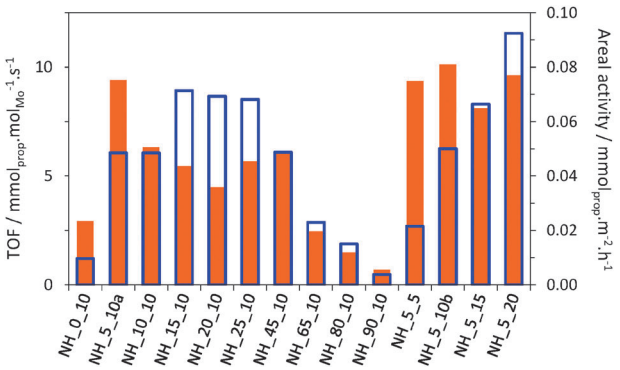

Fig. 6 Metathesis activity after 14 min on stream expressed as turnover frequency, "TOF" (left axis, full bars: mmol of propene converted per mol of Mo per second) or "areal activity" (right axis, empty bars: mmol of propene converted per m^2 of catalyst per hour).

Moreover, the nature of the acid sites is probably affected. To better understand the influence of the Al content and the role of the acidity of the catalysts in the metathesis reaction it would be necessary to differentiate Brönsted and Lewis acidic sites, for instance using adsorption of pyridine and FTIR.

The different NH_5_X catalysts (which have similar specific surface areas) display similar TOF values, around 10 mmol g^{-1} s^{-1}. This confirms the good dispersion of Mo species even at high MoO_3 content, in agreement with XRD and Raman spectroscopy. It suggests that increasing the loading leads to a proportional increase in the active sites density. This was not the case for catalysts prepared by classical impregnation with ammonium heptamolybdate, where the activity did not improve for loadings above *ca.* 8 wt%, due to the formation of crystalline molybdenum oxide and $Al_2(MoO_4)_3$.[11]

One recurrent problem when comparing data from the literature is the disparity in the experimental conditions (activation and reaction) used by different authors to evaluate the activity of different catalysts. Also, activity data can be expressed in many different ways. Here the catalysts can easily be compared with other systems already described by us[4,8,11,13–15] and tested under the exact same experimental conditions (Table 3). The highest performance reported by Handzlik *et al.* (who used very similar conditions) is shown as well. The specific activity of NH_5_20 is more than 2 times higher than that of MoO_3/SiO_2–Al_2O_3 catalysts prepared by optimized impregnation methods[15] or flame spray pyrolysis (FSP).[8]

The TOF values found for the best NH catalysts are around 10 $mmol_{propene}$ mol^{-1}_{Mo} s^{-1}, significantly higher than the values reported for MoO_3/SiO_2–Al_2O_3 catalysts prepared by impregnation methods. Previously reported XPS results[17] showed that migration of Mo species toward the surface took place during calcination of NH catalysts; however, the proportion of Mo atoms at the surface of NH catalysts cannot be higher than in the catalysts prepared by impregnation. Thus, the higher TOF values observed indicate that the MoO_x surface species formed in the non-hydrolytic samples are more active. Indeed, time-of-flight secondary ion mass spectroscopy suggested that highly dispersed Mo (isolated) surface sites were present at the surface of NH catalysts,[17] whereas the catalysts prepared by impregnation contained a significant amount of oligomeric Mo species.

Table 3 Comparison of the catalytic performance of NH catalysts and Si/Al/Mo catalysts prepared by wet impregnation (WI) with different precursors or flame spray pyrolysis (FSP) or thermal spreading (TS)

Catalyst	Mo source	MoO_3 content/ wt%	Specific activity/ mmol g_{cat}^{-1} h^{-1}	TOF/ $mmol_{propene}$ mol_{Mo}^{-1} s^{-1}	Ref.
NH_5_10	$MoCl_5$	9.5	25	10.5	This work[d]
NH_5_20	$MoCl_5$	18.8	45	9.6	This work[d]
WI-AHM	AHM	8.0	12	6.0	11
WI-OXA	AHM[a]	19.2	19	3.9	15
WI-MoH	Mo hydrate	12.9	21	6.5	15
FSP 1	Mo2-EH[b]	1.0	18	71.3	8
FSP 3	Mo2-EH[b]	3.0	9	11.4	8
FSP 5	Mo2-EH[b]	5.0	2	1.9	8
TS-acac[c]	$MoO_2(acac)_2$	2.0	10	20.0	5
TS-MoO_3	MoO_3	11.5	12	4.2	13

[a] With oxalic acid as an additive. [b] Mo2-EH = Mo 2-ethylhexanoate. [c] All catalysts were tested in the same set-up, with exactly the same experimental conditions except "TS-acac", tested by Handzlik *et al.* under similar conditions but not in the same set-up. [d] Activity data published in ref. 17 were underestimated due to diffusional limitations.

An extremely high TOF value (71 $mmol_{propene}$ $mol^{-1}{}_{Mo}$ s^{-1}) was recently reported for a MoO_3/SiO_2–Al_2O_3 catalyst prepared by flame spray pyrolysis with a very low MoO_3 loading (1 wt%).[8] In this case, a clear correlation between the proportion of isolated molybdates and the metathesis activity was established and the activity decreased drastically with the MoO_3 loading: for a 2 wt% MoO_3 loading the TOF value (11.4 $mmol_{propene}$ $mol^{-1}{}_{Mo}$ s^{-1}) becomes comparable to the TOF values found for NH catalysts (Table 3). These results support the idea that highly dispersed, possibly isolated, MoO_x species are the most active metathesis centres, as earlier suggested by Ono *et al.*[48] However, one must keep in mind that the active sites in supported metathesis catalysts represent a very small proportion of the present transition metal atoms.[49]

The outstanding specific activity that can be reached for the optimized NH catalysts would thus result from a combination between their excellent texture and the good dispersion of Mo species even at high Mo contents. Note that high metathesis activity levels were also very recently obtained in the reverse reaction (production of propene from ethene and butene) with aerosol-made catalysts.[16] These systems might compete with NHSG-made catalysts, but proper comparison (in the same reaction and same conditions) is still lacking.

4. Conclusions

An innovative non-hydrolytic sol–gel route has been investigated for the preparation of MoO_3–SiO_2–Al_2O_3 mixed oxides dedicated to the catalysis of light olefin metathesis. This method, based on the etherolysis-condensation of chloride precursors, allows preparing in one step mesoporous mixed oxide samples with well-controlled compositions. Such a sol–gel route differs markedly from classical impregnation methods: instead of depositing a catalytically active phase on a preformed support, the active phase is directly incorporated with the other components of the catalyst. After calcination, well-dispersed MoO_x species are stabilized at the surface of the mixed oxides. The influence of the composition was systematically investigated. The Al_2O_3 content (or Si/Al ratio) strongly influences the texture, the surface acidity and the catalytic performance. Increasing the MoO_3 content and keeping the Si/Al ratio to ~17 allow maintaining the most favourable textural properties and increase the activity of the catalysts. On the basis of specific activity (per mass of catalyst), the best catalysts prepared *via* the non-hydrolytic route are more than two times more active in the self-metathesis of propene than the best MoO_3–SiO_2–Al_2O_3 catalysts prepared *via* other methods (impregnation, flame spray pyrolysis, thermal spreading) reported in the literature.

Experimental section

Catalyst preparation

The non-hydrolytic sol–gel syntheses[23] were performed under an argon atmosphere using a glove box. $SiCl_4$ (Alfa Aesar 99.9%), $AlCl_3$ (Alfa Aesar 99.9%), and $MoCl_5$ (Alfa Aesar 99.6%) were used as received. Diisopropyl ether ($^iPr_2O$) was purchased (Aldrich, 99%) and was further dried by distillation over sodium wire. Table S1 (ESI†) gives the precise amount of reactants involved in each preparation. The chloride precursors were introduced first in an 80 ml Pyrex glass tube or an autoclave, and then the stoichiometric amount of $^iPr_2O$ was added. More precisely, the number of moles of $^iPr_2O$ is calculated so that number of moles of ^iPr groups is equal to the total number of Cl groups in the precursors. In the end, the solvent (CH_2Cl_2) was introduced. The amounts of reactants involved in the preparation of each catalyst are reported in Table S1 (ESI†). The solution obtained was heated at 110 °C for 4 days under autogeneous pressure (*ca.* 0.7 MPa). After cooling to room temperature, the gel was washed with CH_2Cl_2 and dried at 20 °C under vacuum (0.00001 MPa) for 1 h and then for 4 h at 120 °C. The xerogel was then crushed in a mortar and calcined for 5 hours at 500 °C in flowing air (10 ml min^{-1}) leading to white to brown powders. These samples are labelled NH_Y_X, where NH stands for "non-hydrolytic sol–gel", where Y represents the Al_2O_3 weight content (in %) and where X represents the MoO_3 weight content (in %). Actually, in the NH_5_X samples (when the MoO_3 content is varied), the nominal Al_2O_3 content is approximately 5 wt%, because it was chosen to keep the SiO_2/Al_2O_3 ratio constant (~17, as in NH_5_10). The precise nominal Al_2O_3 content is 5.3, 5.0, 4.7 and 4.4 wt% for NH_5_5, NH_5_10, NH_5_15 and NH_5_20 respectively. The preparation of NH_5_10 was done twice and independently to check the reproducibility of the preparation route (samples noted NH_5_10a and NH_5_10b).

Catalyst characterization

The weight percentages of Mo, Si and Al were measured by Inductively Coupled Plasma-Optical Emission Spectrometry (ICP-OES) on an Iris Advantage apparatus from Jarrell Ash Corporation. The materials were dried at 105 °C prior to measurements. N_2 physisorption experiments were performed at −196 °C on a Micromeritics Tristar. The samples were outgassed overnight at 150 °C under vacuum (2 Pa). The specific surface area was determined from the BET method

in the 0.05–0.30 P/P_0 range. The pore size distribution was derived from the desorption branch using the BJH method. The average pore diameter is calculated as (4 × pore volume/BET specific surface area). The micropore volume was estimated using *t*-plot analysis in the 0.35–0.05 nm range. X-Ray diffraction (XRD) measurements were performed on the fresh catalysts with a Siemens D5000 diffractometer using the Kα radiation of Cu (λ = 1.5418 Å). The 2θ range was recorded between 5° and 75° at a rate of 0.02° s^{-1}. The ICDD-JCPDS database was used to identify the crystalline phases. Raman characterization was done on the InVia Raman microscope (Renishaw) equipped with a diode light (785 nm). Resolution was set to 4 cm^{-1}. Acquisition time was 10 s and 10 scans were recorded and averaged for each sample. The acidity was evaluated by NH_3-temperature programmed desorption (NH_3-TPD) on a Micromeritics AutoChem 2910 apparatus with a thermal conductivity detector (TCD). A 100 mg sample was preheated in helium at 500 °C for 60 min (ramp 10 °C min^{-1}). Adsorption of NH_3 (5 vol% in helium; flow rate 30 ml min^{-1}) was done at 100 °C for 45 min. Physisorbed NH_3 was removed by purging with helium at 100 °C for 1 hour (flow rate 30 ml min^{-1}). The TPD measurement was conducted by heating the sample from 100 to 500 °C at a 10 °C min^{-1} rate.

Metathesis reaction

The activity of the catalysts in the self-metathesis of propene was measured in a multi-channel apparatus which allows fully automated control of gas flows and of three temperature zones (gas pre-heating, reactor, and post reactor lines with 16-port valve) along with reactor switching and product sampling.[50] All catalysts were sieved and selected in the 200–315 μm granulometric size range. The catalysts (200 mg or 100 mg for the most active samples, NH_5_10, NH_5_15 and NH_5_20) were introduced in quartz straight reactors (5 mm i.d.). Prior to reaction, the catalysts were activated by heating up to 550 °C (temperature ramp of 5 °C min^{-1}) in N_2 (14 ml min^{-1} flow in each reactor) and keeping this temperature for 2 h. Afterwards the system was cooled down to the reaction temperature (40 °C) under the same N_2 flow. The reaction was carried out at 40 °C in a propene and N_2 flow (90 : 10 vol.%) of 8 ml min^{-1}. Propene (99.95% purity) and N_2 (99.995% purity) were further purified over Molsieve 3A (Roth) filters. N_2 was also purified by an oxygen filter (Oxysorb-glass, Linde). The composition of the reaction gas was analysed by an Agilent 6890 GC. The separation of hydrocarbons was performed on a HP-AL/M column (30 m length, 0.53 mm i.d., 0.15 μm film thickness) by applying a temperature ramp between 90 and 140 °C and FID detection. Product analysis took about 6.5 min for each injection. N_2, used as an internal standard, was analysed on a HP Plot-Q column with TCD detection. The experiments were carried out at atmospheric pressure. Under these experimental conditions, the selectivity to metathesis products always proved to be close to 100% (typically 99%). Only traces of secondary metathesis products (1-butene, pentenes, and hexenes) and isomerization products (isobutene) were detected. The activity was calculated on the basis of metathesis products (ethene and *trans*- and *cis*-butene) formation. The specific activity was defined as the number of moles of propene converted to metathesis products per gram of catalyst and per hour. The apparent turnover frequency (TOF) is defined as the number of moles of propene converted per mole of Mo (considering the total bulk Mo content) and per second. The areal activity was defined as the number of moles of propene converted to metathesis products per square metre of catalyst and per hour. The standard deviation for activity measurements was less than 3%.

Acknowledgements

The authors from ICG acknowledge the Ministère de l'Enseignement Supérieur et de la Recherche and the Centre National de la Recherche Scientifique (CNRS) in France for financial support. D.P.D. thanks the FNRS for his Research Fellow and Postdoctoral Researcher positions. The authors from UCL are involved in the "Inanomat" IUAP network (Service public fédéral de programmation politique scientifique, Belgium), in the Cost Action D41 (European Science Foundation) and in the European Multifunctional Material Institute (EMMI) built on the basis of the former "FAME" Network of Excellence, EU 6th FP.

Notes and references

1 J. C. Mol, *J. Mol. Catal. A: Chem.*, 2004, **213**, 39–45.
2 R. L. Banks and G. C. Bailey, *Ind. Eng. Chem. Prod. Res. Dev.*, 1964, **3**, 170–173.
3 H. Liu, L. Zhang, X. Li, S. Huang, S. Liu, W. Xin, S. Xie and L. Xu, *J. Nat. Gas Chem.*, 2009, **18**, 331–336.
4 D. P. Debecker, D. Hauwaert, M. Stoyanova, A. Barkschat, U. Rodemerck and E. M. Gaigneaux, *Appl. Catal., A*, 2011, **391**, 78–85.
5 J. Handzlik, J. Ogonowski, J. Stoch, M. Mikolajczyk and P. Michorczyk, *Appl. Catal., A*, 2006, **312**, 213–219.
6 J. Handzlik, J. Ogonowski, J. Stoch and M. Mikolajczyk, *Catal. Lett.*, 2005, **101**, 65–69.
7 H. Aritani, O. Fukuda, T. Yamamoto, T. Tanaka and S. Imamura, *Chem. Lett.*, 2000, 66–67.
8 D. P. Debecker, B. Schimmoeller, M. Stoyanova, C. Poleunis, P. Bertrand, U. Rodemerck and E. M. Gaigneaux, *J. Catal.*, 2011, **277**, 154–163.
9 J. Handzlik, J. Ogonowski, J. Stoch and M. Mikolajczyk, *Appl. Catal., A*, 2004, **273**, 99–104.
10 X. Li, W. Zhang, S. Liu, L. Xu, X. Han and X. Bao, *J. Phys. Chem. C*, 2008, **112**, 5955–5960.
11 D. P. Debecker, M. Stoyanova, U. Rodemerck, A. Leonard, B.-L. Su and E. M. Gaigneaux, *Catal. Today*, 2011, **169**, 60–68.
12 X. Li, W. Zhang, S. Liu, X. Han, L. Xu and X. Bao, *J. Mol. Catal. A: Chem.*, 2006, **250**, 94–99.
13 D. P. Debecker, M. Stoyanova, U. Rodemerck, P. Eloy, A. Léonard, B.-L. Su and E. M. Gaigneaux, *J. Phys. Chem. C*, 2010, **114**, 18664–18673.
14 D. P. Debecker, M. Stoyanova, U. Rodemerck and E. M. Gaigneaux, *Stud. Surf. Sci. Catal.*, 2010, **175**, 581–585.
15 D. P. Debecker, M. Stoyanova, U. Rodemerck and E. M. Gaigneaux, *J. Mol. Catal. A: Chem.*, 2011, **340**, 65–76.
16 D. P. Debecker, M. Stoyanova, F. Colbeau-Justin, U. Rodemerck, C. Boissière, E. M. Gaigneaux and C. Sanchez, *Angew. Chem., Int. Ed.*, 2012, DOI: 10.1002/anie.201106277.
17 D. P. Debecker, K. Bouchmella, C. Poleunis, P. Eloy, P. Bertrand, E. M. Gaigneaux and P. H. Mutin, *Chem. Mater.*, 2009, **21**, 2817–2824.
18 A. Baiker, J.-D. Grunwaldt, C. A. Mueller and L. Schmid, *Chimia*, 1998, **52**, 517–524.
19 R. D. Gonzalez, T. Lopez and R. Gomez, *Catal. Today*, 1997, **35**, 293–317.
20 J. Livage, *Catal. Today*, 1998, **41**, 3–19.

21 C. Sanchez, L. Rozes, F. Ribot, C. Laberty-Robert, D. Grosso, C. Sassoye, C. Boissiere and L. Nicole, *C. R. Chim.*, 2010, **13**, 3–39.
22 D. C. M. Dutoit, M. Schneider and A. Baiker, *J. Catal.*, 1995, **153**, 165–176.
23 A. Vioux, *Chem. Mater.*, 1997, **9**, 2292–2299.
24 P. H. Mutin and A. Vioux, *Chem. Mater.*, 2009, **21**, 582–596.
25 A. M. Cojocariu, P. H. Mutin, E. Dumitriu, F. o. Fajula, A. Vioux and V. Hulea, *Chem. Commun.*, 2008, 5357–5359.
26 O. Lorret, V. Lafond, P. H. Mutin and A. Vioux, *Chem. Mater.*, 2006, **18**, 4707–4709.
27 P. Moggi, M. Devillers, P. Ruiz, G. Predieri, D. Cauzzi, S. Morselli and O. Ligabue, *Catal. Today*, 2003, **81**, 77–85.
28 P. H. Mutin, A. F. Popa, A. Vioux, G. r. Delahay and B. Coq, *Appl. Catal., B*, 2006, **69**, 49–57.
29 A. F. Popa, P. H. Mutin, A. Vioux, G. Delahay and B. Coq, *Chem. Commun.*, 2004, 2214–2215.
30 A. G. Fisch, N. S. M. Cardozo, A. R. Secchi, F. C. Stedile, P. R. Livotto, D. S. de Sa, Z. N. da Rocha and J. H. Z. dos Santos, *Appl. Catal., A*, 2009, **354**, 88–101.
31 J. Zhu, J. Yang, Z. F. Bian, H. Ren, Y. M. Liu, Y. Cao, H. X. Li, H. Y. He and K. N. Fan, *Appl. Catal., B*, 2007, **76**, 82–91.
32 D. P. Debecker, R. Delaigle, K. Bouchmella, P. Eloy, E. M. Gaigneaux and P. H. Mutin, *Catal. Today*, 2010, **157**, 125–130.
33 D. P. Debecker, K. Bouchmella, R. Delaigle, P. Eloy, C. Poleunis, P. Bertrand, E. M. Gaigneaux and P. H. Mutin, *Appl. Catal., B*, 2010, **94**, 38–45.
34 A. N. Desikan, L. Huang and S. T. Oyama, *J. Phys. Chem.*, 1991, **95**, 10050–10056.
35 X. Carrier, E. Marceau and M. Che, *Pure Appl. Chem.*, 2006, **78**, 1039–1055.
36 H. C. Hu, I. E. Wachs and S. R. Bare, *J. Phys. Chem.*, 1995, **99**, 10897–10910.
37 G. Mestl and T. K. K. Srinivasan, *Catal. Rev. Sci. Eng.*, 1998, **40**, 451–570.
38 O. Collart, P. Van der Voort, E. F. Vansant, E. Gustin, A. Bouwen, D. Schoemaker, R. R. Rao, B. M. Weckhuysen and R. A. Schoonheydt, *Phys. Chem. Chem. Phys.*, 1999, **1**, 4099–4104.
39 H. Jeziorowski, H. Knozinger, P. Grange and P. Gajardo, *J. Phys. Chem.*, 1980, **84**, 1825–1829.
40 N. Katada, H. Igi, J. H. Kim and M. Niwa, *J. Phys. Chem. B*, 1997, **101**, 5969–5977.
41 L. Rodriguez-Gonzalez, F. Hermes, M. Bertmer, E. Rodriguez-Castellon, A. Jimenez-Lopez and U. Simon, *Appl. Catal., A*, 2007, **328**, 174–182.
42 R. E. Sempels and P. G. Rouxhet, *J. Colloid Interface Sci.*, 1976, **55**, 263–273.
43 P. O. Scokart, F. D. Declerck, R. E. Sempels and P. G. Rouxhet, *J. Chem. Soc., Faraday Trans. 1*, 1977, **73**, 359–371.
44 S. Rajagopal, J. A. Marzari and R. Miranda, *J. Catal.*, 1995, **151**, 192–203.
45 B. Zhang, N. Liu, Q. Lin and D. Jin, *J. Mol. Catal.*, 1991, **65**, 15–28.
46 A. N. Desikan, W. M. Zhang and S. T. Oyama, *J. Catal.*, 1995, **157**, 740–748.
47 H. Aritani, O. Fukuda, A. Miyaji and S. Hasegawa, *Appl. Surf. Sci.*, 2001, **180**, 261–269.
48 T. Ono, M. Anpo and Y. Kubokawa, *J. Phys. Chem.*, 1986, **90**, 4780–4784.
49 J. Handzlik and J. Ogonowski, *Catal. Lett.*, 2003, **88**, 119–122.
50 U. Rodemerck, P. Ignaszewski, M. Lucas and P. Claus, *Chem. Eng. Technol.*, 2000, **23**, 413–416.